

Complex Refraction Metasurfaces for Locally Enhanced Propagation Through Opaque Media

Sinuhé Perea-Puente and Francisco J. Rodríguez-Fortuño*

Metasurfaces with linear phase gradients can redirect light beams. Controlling both phase and amplitude of a metasurface is proposed to extend Snell's law to the realm of complex angles, enabling a non-decaying transmission through opaque media with complex refractive indices. This leads to the discovery of non-diffracting and non-decaying solutions to the wave equation in opaque media, in the form of generalized cosine and Bessel-beams with a complex argument. While these solutions present nonphysical exponentially growing side tails, this is addressed via a windowing process, removing the side tails of the field profile while preserving significant transmission enhancement through an opaque slab on a small localized region. Such refined beam profiles may be synthesized by passive metasurfaces with phase and amplitude control at the opaque material's interface. The findings, derived from rigorous solutions of the wave equation, promise new insights and enhanced control of light propagation in opaque media.

Metasurfaces are two-dimensional (2D) engineered structures^[9–13] whose meta-atoms may control, locally, the amplitude, and phase of the transmitted or reflected fields. Linear phase gradient metasurfaces are equivalent to adding a real transverse wave-vector component to a transmitted beam, enabling beam redirection and generalizing Snell's Law.^[14–16] We raise the possibility of achieving a complex-valued additive transverse wave-vector to enable greater control. A complex wave-vector (with simultaneous non-zero real and imaginary parts) corresponds to a linear phase gradient simultaneous with an exponentially decaying amplitude profile. This further generalizes Snell's law to complex angles, enabling surprising possibilities. Metasurfaces with simultaneous control

1. Introduction

Propagation through a medium that would normally block, absorb, interfere or distort the passage of incident electromagnetic waves is a sought-after phenomenon, with the intriguing promise of enabling “seeing through walls”. Recent research works have reported such phenomena in different contexts by using several alternative methods, such as propagation through scattering media using speckle correlations,^[1] scattering-invariant modes,^[2] propagation through lossy materials by complex wave-vector engineering,^[3–5] propagation through layered Bragg media within forbidden bands using spatial shaping,^[6] non-Hermitian exceptional points,^[7] or exploiting parity-time-symmetry in evanescent waves,^[8] among others.

of amplitude and phase of a wave are generally known as “holographic” metasurfaces^[17] and are attainable in the optical domain with designs ranging from metallic unit cells^[18] to all-dielectric meta-atoms.^[19] A fine control of both amplitude and phase has also been experimentally achieved in radiofrequencies and microwaves.^[20]

A particularly tough challenge is to achieve transmission of monochromatic light through an opaque medium modeled by a uniform isotropic complex refractive index $n = \sqrt{\epsilon\mu} = n' + in''$ with a non-vanishing imaginary part. Inside such a medium, the momentum eigenmode solutions to the wave-equation, whose spatial dependence is given by an exponential $e^{i\mathbf{k}\cdot\mathbf{r}}$, exist under the condition that the wave-vector \mathbf{k} must be complex, owing to the Helmholtz equation $\nabla^2\mathbf{E}(\mathbf{r}) + (nk_0)^2\mathbf{E}(\mathbf{r}) = 0$, which under the exponential ansatz leads to the dispersion relation $\mathbf{k}\cdot\mathbf{k} = k_x^2 + k_y^2 + k_z^2 = (nk_0)^2$ (see [Supporting Information](#)). This implies that $\mathbf{k} = \mathbf{k}' + i\mathbf{k}''$ has simultaneously non-zero real and imaginary vector parts, so the spatial dependence of the wave explicitly becomes $e^{i\mathbf{k}'\cdot\mathbf{r}} \cdot e^{-\mathbf{k}''\cdot\mathbf{r}}$ associated with an unavoidable exponential decay following the direction of the imaginary term \mathbf{k}'' , corresponding to an inhomogeneous wave. Conventionally, this attenuation profile happens in the direction of penetration inside the material, causing exponential attenuation through the medium. However, this must not always be the case. Maxwell's equations allow freedom regarding the direction in which waves may be attenuated. Indeed, in refs. [3, 4] it was found theoretically and recently confirmed experimentally,^[5] that propagation inside an opaque medium exhibits deeply penetrating waves, by tuning the imaginary wave-vector component \mathbf{k}'' to be orientated

S. Perea-Puente, F. J. Rodríguez-Fortuño
Department of Physics
King's College London
Strand, London WC2R 2LS, United Kingdom
E-mail: francisco.rodriguez_fortuno@kcl.ac.uk

S. Perea-Puente, F. J. Rodríguez-Fortuño
London Centre for Nanotechnology
17-19 Gordon Street, London WC1H 0AH, United Kingdom

 The ORCID identification number(s) for the author(s) of this article can be found under <https://doi.org/10.1002/lpor.202300867>

© 2024 The Authors. Laser & Photonics Reviews published by Wiley-VCH GmbH. This is an open access article under the terms of the [Creative Commons Attribution](#) License, which permits use, distribution and reproduction in any medium, provided the original work is properly cited.

DOI: 10.1002/lpor.202300867

parallel to the incident interface, obtaining only a purely real component of $\mathbf{k} \cdot \hat{\mathbf{u}}$ in the direction $\hat{\mathbf{u}}$ that penetrates the opaque material. This was proposed by illuminating the opaque media from lossless free space with inhomogeneous waves, such as those coming from a leaky waveguide, at carefully engineered angles.^[3,4] In this work, we propose achieving the desired wave-vectors using metasurfaces, greatly inspired by its diffraction features, but extending the concept of phase gradients into a phase-and-amplitude profile which effectively translates into complex wave-vector contributions. We also expand the family of solutions that propagate diffractionlessly inside an opaque medium, beyond a single inhomogeneous wave, to include the cosine and Bessel beams family.

Let's explore from first principles the limitations and constraints imposed by Maxwell's equations of electromagnetism inside an opaque material, in a general case. Without loss of generality, we choose our axes such that the axis z is oriented in the direction in which we want to penetrate the material (for instance, normal to the surface of a slab of opaque material that we want to "see" through). Can we find waves that deeply propagate into an opaque material, with no exponential attenuation in the desired z -direction? The spatial dependence of the wave in that direction is given by k_z . We know from the dispersion relation $\mathbf{k} \cdot \mathbf{k} = k_x^2 + k_y^2 + k_z^2 = (nk_0)^2$ that

$$k_z = \left[(nk_0)^2 - k_x^2 - k_y^2 \right]^{1/2} = \left[(nk_0)^2 - k_t^2 \right]^{1/2} \quad (1)$$

where k_t is often called the transverse wavenumber.^[21] The above equation is often expressed in terms of the transmitted angle θ , via $k_t = nk_0 \sin \theta$ and $k_z = nk_0 \cos \theta$. In a lossy or opaque material, $nk_0 = (n' + in'')k_0$ corresponds to a complex number, which in general suggests that $k_z = nk_0 \cos \theta$, being proportional to a complex n , must have an imaginary component too. A complex k_z with non-zero imaginary part gives rise to the attenuation profile characteristic of the Beer-Lambert law in an opaque material. However, this is not necessarily the case. The transverse components k_x and k_y (and hence k_t and θ) may also be complex numbers, corresponding to complex refraction angles. Complex refraction angles are a known mathematical concept that allows modeling amplitude decay in addition to phase advance,^[22,23] but with no easy geometrical interpretation. The product of two complex numbers can be real under certain conditions, hence the complex-valued angle θ can be fine-tuned such that $\cos \theta$ perfectly counterbalances the imaginary part of nk_0 to achieve a purely real product $k_z = nk_0 \cos \theta$, and hence a non-attenuating transmission in the z -direction. Following Equation (1), this corresponds to finding a complex $(k_t)^2$ to cancel out the imaginary part of $(nk_0)^2$. This was precisely the active approach exploited in refs. [3, 4]. Here, we propose achieving the required complex k_t by using a passive metasurface.

Metasurfaces are an established method to engineer the transverse wave-vector of an impinging wave by means of phase gradients. For this purpose, consider a metasurface on an interface $z = 0$; if this metasurface introduces a spatially varying transmission phase gradient Φ that has a linear dependence in some direction on the xy plane, $\Phi(x, y) = \Delta k_x x + \Delta k_y y$, then the effective transmission coefficient is $t(x, y) \propto e^{i\Phi} = e^{i(\Delta k_x x + \Delta k_y y)}$, such that

any incident wave $E_{\text{inc}}(z = 0) \propto e^{ik_x x + ik_y y}$ will acquire an additional phase upon transmission according to the following expression:

$$E_t(z = 0) = t(x, y) E_{\text{inc}}(z = 0) \propto t(x, y) e^{ik_x x + ik_y y} \propto e^{i(k_x + \Delta k_x)x + i(k_y + \Delta k_y)y} \quad (2)$$

which is mathematically equivalent to a change in the incident transverse wave-vector $(k_x, k_y) \rightarrow (k_x + \Delta k_x, k_y + \Delta k_y)$, i.e. $\mathbf{k}_t \rightarrow \mathbf{k}_t + \Delta \mathbf{k}_t$. This method was used as a generalization of Snell's law of refraction ref. [14] and gave rise to many applications of metasurfaces for flat lensing and beam steering.^[15,16]

As is well known, conventional refraction at a smooth boundary between two materials ultimately stems from the conservation of the transverse wave-vector in the interface. By k_x and k_y being conserved between the incident and transmitted waves, we can derive from Equation (1) that k_z must be genuinely different in each medium, according to their different refractive index n , giving rise to the angles of incidence and refraction of the wave, summarized in Snell-Descartes' law, **Figure 1a**. While this formula is typically used in the context of transparent materials with both real refractive indexes simultaneously, the conservation of the transverse momentum argument always applies. If n is complex in the second medium, k_x and k_y being the transverse components in this interface are still conserved, and hence will be real because the incident wave comes from a transparent medium, and so then k_z will be complex, resulting in an attenuation into the second medium, as shown in **Figure 1b**. The use of a metasurface breaks the requirement of conservation of transverse momentum, by breaking the translational symmetry of the interface. Indeed, a metasurface with a linear phase gradient permits effective additive changes to the transmitted transverse wave-vector as described above, $(k_x, k_y) \rightarrow (k_x + \Delta k_x, k_y + \Delta k_y)$, achieving the corresponding change in angle, generalising Snell's law,^[14] corresponding to **Figure 1c**.

Here, we propose to further generalize the change in transverse wave-vector in the transmitted wave, not limiting ourselves to changing the angle of transmission, but instead including complex values into $\Delta \mathbf{k}_t$ such that $(k_x, k_y) \rightarrow (k_x + \Delta k_x, k_y + \Delta k_y) = (k_x + \Delta k'_x + i\Delta k''_x, k_y + \Delta k'_y + i\Delta k''_y)$. In order to achieve this, one only needs the transmission coefficient to be $t \propto e^{i\Delta k_x x + i\Delta k_y y} = e^{i(\Delta k'_x x + \Delta k'_y y)} e^{-(\Delta k''_x x + \Delta k''_y y)}$, which represents a simultaneous phase $\arg(t)$ and amplitude $|t|$ control. By doing this, k_x and k_y can be simultaneously engineered by the metasurface at will, to attain any complex value. This is mathematically equivalent to complex-valued angles of refraction, thus representing a complex refraction metasurface. Specifically, the complex k_x and k_y may be engineered in such way to obtain a real-valued k_z , even inside a lossy or opaque material, and therefore achieving deep perfect penetration inside the material. Note that the engineering of the transverse wave-vector can be achieved for any angle of incidence, including normal incidence of a plane wave on the interface, as shown in **Figure 1d**.

In fact, **Figure 1d** demonstrates how, by adding an exponential amplitude dependence to the field profile along the x axis, k_z can be made purely real, resulting in transmission with no attenuation along the z -axis. Of course, attenuation is still present on this opaque material, but it is happening along the x - rather than the z -direction into which we want to penetrate. In essence, the

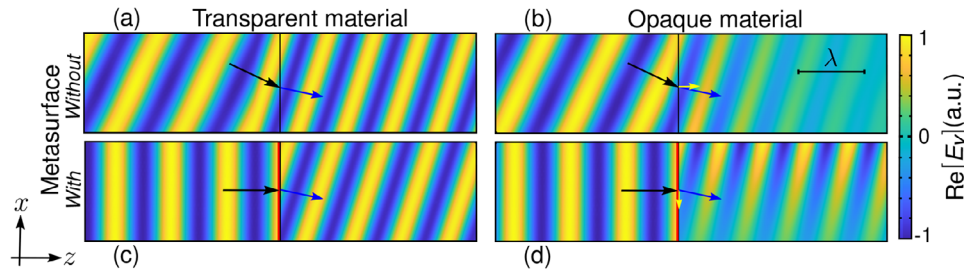


Figure 1. Descartes-Snell law in transparent and opaque materials. Electric field (real part of TE electric field component) at a smooth interface transitioning from free space to a transparent (a,c) or an opaque (b,d) material. The two scenarios considered involve the absence (a,b) and presence (c,d) of a metasurface designed to modify the transmitted wave-vector. In the transparent case (a,c), the effective refractive index of the transmitted material is $n = 1.4$, while in the opaque scenario (b,d), the material has a complex refractive index of $n = 1.4 + 0.15i$. In (a), an obliquely incident wave refracts upon entering a transparent material, demonstrating Snell's law and conservation of transverse momentum. Next, in (b) an obliquely incident wave refracts and experiences attenuation upon entering an opaque material. The imaginary component of the wave-vector points along z due to conservation of transverse momentum $k_x \in \mathbb{R}$. Now in (c) a normally incident wave refracts into a transparent material, at the same angle as in (a), thanks to the interaction with a designer phase gradient metasurface with transmission coefficient $t \propto e^{i\Delta k_x x}$ that induces a synthetic transverse wave-vector Δk_x . In (d) a normally incident wave interacts with a phase-and-amplitude metasurface with transmission coefficient $t \propto e^{i(\Delta k_x' + i\Delta k_x'')x} = e^{i\Delta k_x' x} e^{-\Delta k_x'' x}$ which synthesises a complex transverse wave-vector $\Delta k_x'$ + $i\Delta k_x''$ (with real and imaginary components, associated to the phase and amplitude of the metasurface, respectively). The metasurface in (d) is designed such that the resulting wave-vector is real along the penetrating z direction, $k_z \in \mathbb{R}$, achieving invariant propagation inside the opaque material. Incident wave-vector (black arrow), real (blue), and imaginary (yellow) components of the transmitted wavenumber are shown as vectors. Colour scale (arbitrary units) is shared for all plots.

use of the “complex-value” metasurface allows us to manually select the direction in which the evanescent decay of the amplitude will occur.

2. Analytical Derivation

Emphasis on the complex nature of the wave equation will be the starting point of this derivation; by looking at Equation (1) we can explicitly find the value that k_t needs to attain in order to achieve a purely real k_z even when $n = n' + in''$ is a complex quantity. For this to happen, two conditions must be simultaneously fulfilled by the argument of the square root in Equation (1): first, we need that $\text{Im}(k_z^2) = 0$, and second $\text{Re}(k_z^2) > 0$. These two hyperbolic conditions guarantee a real k_z . It is straightforward to show that the first rectangular condition leads to $k_t' k_t'' = n' n''$, while the second inequality is equivalent to $k_t'^2 - k_t''^2 < k_0^2 (n'^2 - n''^2)$. Now, the conic solutions for k_t are not unique; there is a full range of values of optimized complex k_t^{opt} solutions fulfilling these two conditions simultaneously. The geometrical characterization of these two conditions on the complex k_t plane is available in the Supporting Information. The family of solutions can be written as an explicit expression with a free real parameter f corresponding to a single degree of freedom such that:

$$k_t^{\text{opt}} = k_0 \underbrace{\left(n' f + i \frac{n''}{f} \right)}_{n \sin(\theta_{\text{opt}})} \quad (3)$$

where $\theta_{\text{opt}} = \sin^{-1}(k_t^{\text{opt}}/nk_0)$ represents the complex angle of refraction. Under this finely tuned condition, substituting Equation (3) into Equation (1), the value of k_z reduces to a purely real value analytically given by $k_z = \frac{k_0}{|f|} \sqrt{(1-f^2)(n'^2 + n''^2 f^2)}$, achieving no exponential decay along z , as initially desired. This of course comes at the cost of having a fully complex k_t that requires

exponential decay (and increase) of the amplitude in the transverse plane. A metasurface with complex $(\Delta k_x, \Delta k_y)$ can be used to generate the required k_t for any incident wave.

An obvious question that arises when looking at this technique is where does the energy come from, to achieve constant field amplitude along z , given that the material may be actively absorbing energy. The answer is to be found by looking at the Poynting vector (black arrows in Figure 2a). The energy lost in absorption is replaced by the energy coming from the edges where the field profile blows up in amplitude. This is in accordance with Poynting's theorem: any absorption at a point is exactly accounted via a net influx of power into that point. This is analytically proven in the Supporting Information. At first sight, therefore, it seems that this technique should be impossible to implement in practice, because an exponentially growing diverging amplitude would need to be attained by the metasurface as $x \rightarrow \infty$, suggesting that an active metasurface with ever-increasing gain would be required. This problem will later be alleviated using passive metasurfaces in which the required transmission profile is windowed in space, such that the transmission coefficient remains always lower than unity. This windowing process locally and partially preserves the non-decaying effect. Before delving into the windowed case, let's first try to understand the ideal “active” case, in which the metasurface exhibits an idealized exponentially growing transmission.

Let's begin with a 2D problem, where $k_y = 0$, and where a transverse electric polarization is assumed $\mathbf{E}(\mathbf{r}) = E_y(\mathbf{r})\mathbf{y}$. In this case, after interaction with the metasurface, we want to achieve a transverse wavenumber $k_x = k_x^{\text{inc}} + \Delta k_x = k_t^{\text{opt}}$ that matches the optimal condition of Equation (3), such that k_z is a purely real value inside the opaque material. This can clearly be achieved if a normally incident plane wave in free space ($k_x^{\text{inc}} = 0$) of amplitude E_{inc} interacts with a metasurface whose transmission coefficient equals $t = e^{i k_t^{\text{opt}} x}$ (which will involve both phase and amplitude changes in accordance to the real and imaginary parts of k_t^{opt}). This metasurface will result in a transmitted field profile

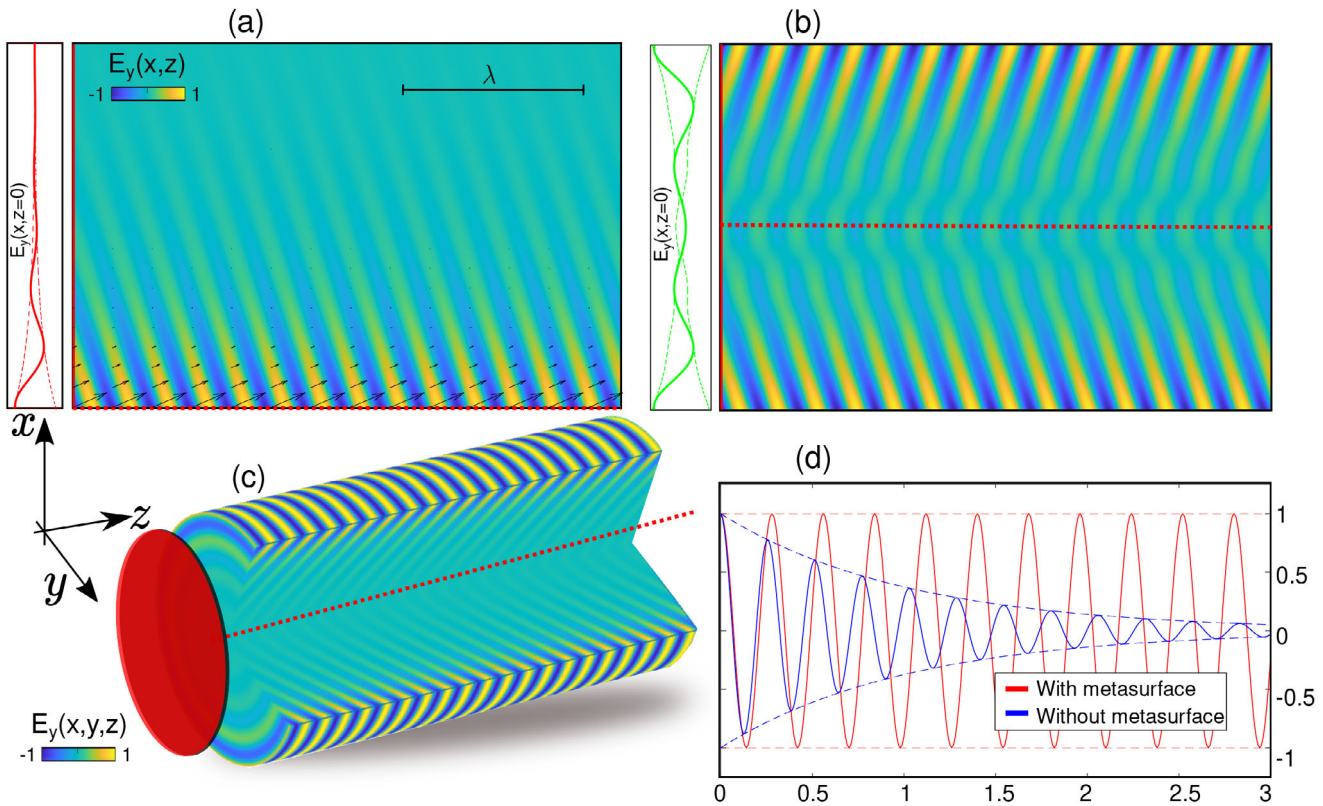


Figure 2. Idealized field profiles and non-decaying profile. Electric field evolution inside an opaque material when designed electric field boundary conditions are placed at $z = 0$ (i.e., metasurface) for different incident profiles. a) A complex- k_x plane wave $E_y(x) = e^{ik_x^{\text{opt}}x}$, b) a complex-argument cosine beam $E_y(x) = \cos(k_t^{\text{opt}}x)$, and c) a complex-argument Bessel beam $E_y(\rho) = J_0(k_t^{\text{opt}}\rho)$ (see exact derivation in Supporting Information). The three are examples of propagation-invariant and diffractionless beams through an opaque material with refractive index $n = 3.8823 + 0.01564i$, corresponding to silicon at HeNe laser wavelength $\lambda = 633\text{nm}$.^[24] The structured electric field at $z = 0$ (which in principle could be synthesized with a metasurface) follows the equations given in the main text with complex transverse wave-vectors, and with fixed parameter $f = 0.11$. In boxes, the initial structured profiles $E_{\text{inc}}(z = 0)$ real part (continuous line) and amplitude (dashed line) are shown. In (d) the field propagation profile along the z axis is shown, observing a constant amplitude (dashed line) and non-decaying harmonic oscillation (real part, continuous line) in the center of the transmitted beam, compared to the decaying profile of the case without metasurface (black) when $E_{\text{inc}}(z = 0) = 1$ is a normally incident plane wave with no structuring. The real part of the time-averaged Poynting vector is also shown in (a) as black arrows. Colour scale (in a. u.) is shared for all plots.

at $z = 0$ equal to $\mathbf{E}(x, z = 0) = \mathbf{E}_{\text{inc}}t = E_{\text{inc}}e^{ik_t^{\text{opt}}xy}$. This field profile induced at the interface $z = 0$ will now propagate inside the opaque material in accordance to Equation (1). When propagated along z using the transfer function $e^{ik_z z}$, with now a purely real k_z (as corresponds to k_t^{opt} by construction), this will result in a transmitted field $\mathbf{E}(x, z) = E_{\text{inc}}e^{i(k_t^{\text{opt}}x + k_z z)y}$. This is an inhomogeneous plane wave whose amplitude $|\mathbf{E}(t)|$ does not decay with z . This idealized case is illustrated in Figure 2a, where for illustration purposes we chose an opaque silicon material at a HeNe laser wavelength. The figure also displays the real Poynting vector as black arrows, showing that the energy indeed comes from the regions of high amplitude at the bottom, in order to sustain the constant amplitude that is achieved along z for every line of constant x .

Interestingly, a single exponential solution (inhomogeneous plane wave) as shown in Figure 2a is not the only possibility that could exhibit this property. In fact, there are many valid values of k_t^{opt} that achieve a real value of k_z , as described by the free parameter f in Equation (3), and thanks to linearity of the

solutions, any combination of valid exponentials with different f values will still be a penetrating solution with no attenuation along z . More simply, however, we can consider by symmetry the combination of two solutions as in Figure 2a but with opposite signs in $k_x = \pm k_t^{\text{opt}}$. Both solutions will have the same real k_z and hence the following field distribution is obtained: $\mathbf{E}(x, z) = E_{\text{inc}}[e^{i(k_t^{\text{opt}}x + k_z z)} + e^{i(-k_t^{\text{opt}}x + k_z z)}]y = 2E_{\text{inc}}\cos(k_t^{\text{opt}}x)e^{ik_z z}y$. This field, invariant in z and thus penetrating, simply requires establishing a cosine-like field profile at $z = 0$. In transparent media this is the well-known 2D non-diffracting cosine beam.^[25–27] In the case of opaque materials, however, we have the intriguing property that k_t^{opt} , and hence the argument of the cosine function, is a complex number. We call this a complex-argument cosine beam. This can be achieved with the metasurface by tuning both the amplitude and phase of the transmission coefficient following $t \propto \cos(k_t^{\text{opt}}x)$. Not surprisingly, like the individual exponential solutions, the cosine profile $\cos(k_t^{\text{opt}}x)$ blows up in amplitude when $x \rightarrow \pm\infty$. Considering this idealized case, the cosine beam indeed propagates arbitrarily deep into the opaque material as shown in Figure 2b.

This time, energy is coming from both top and bottom, to allow for the non-decaying propagation along z in the center. Other relative amplitudes of the two exponentials could be considered, giving rise to sine beams or any other arbitrary function by careful Fourier decomposition.

Finally, we consider three-dimensional (3D) solutions. We can produce a linear superposition of complex exponentials whose transverse wave-vector $k_x\hat{x} + k_y\hat{y}$ points in every possible direction on the xy -plane, while still maintaining the same transverse wave-number $k_t^{\text{opt}} = (k_x^2 + k_y^2)^{1/2}$ by taking $k_x = k_t^{\text{opt}} \cos(\alpha)$ and $k_y = k_t^{\text{opt}} \sin(\alpha)$, with $\alpha \in [0, 2\pi)$. This forms a 3D Bessel beam, but with the peculiarity that k_t is complex, and hence the Bessel functions that describe the field distribution have complex valued arguments in the family $J_m(k_t, \rho)$, where $\rho = \sqrt{x^2 + y^2}$ is the cylindrical radial coordinate and J_m is the Bessel function of first kind and order m . There is freedom on m and on the polarizations of the different plane wave components in 3D, which adds much variety and complexity to the mathematics of the solution, described in detail in the Supporting Information; as a simplest example, the electric field corresponding to a y -polarized Bessel beam is given by $\mathbf{E}(\mathbf{r}) = E_{\text{inc}}[k_z J_0(k_t^{\text{opt}} \rho) \mathbf{y} - ik_t^{\text{opt}} J_1(k_t^{\text{opt}} \rho) \sin(\phi) \mathbf{z}] e^{ik_z z}$, a full solution to Maxwell's equations, and its y -component is depicted in Figure 2c. This is indeed the generalization, to opaque materials, of the well known diffractionless Bessel beams defined in transparent materials. In our case, the argument of the Bessel functions (k_t, ρ) forming the beam is complex, so the amplitude of the beam grows with ρ , but the beam is still invariant with z , despite the material being opaque.

As we have mentioned before, the obvious caveat of the phenomenon presented here is that an infinite exponential increase in the amplitude of the transmission along the direction parallel to the interface is needed, thus requiring an infinite energy to maintain the propagated beam in a physical realization. To avoid this unphysical scenario, we next study the effect of spatially windowing the initial excitation, with a hope of still achieving non-decaying transmission far from the edges, thanks to the locality of Maxwell equations. This is discussed in the following section.

3. Finite Case: Bullseye Metasurface

Let us avoid the infinitely growing tails of the complex-argument cosine and Bessel beams by windowing the initial field profile at $z = 0$ using the following expression:

$$\mathbf{E}_{\text{windowed}}(x, z = 0) = E_{\text{inc}} \frac{w(x)\mathbf{E}_{\text{ideal}}(x, z = 0)}{\max(|w(x)\mathbf{E}_{\text{ideal}}|)} \quad (4)$$

where $\mathbf{E}_{\text{ideal}}(x, z = 0)$ corresponds to any of the exponentially growing profiles shown in the previous section (Figure 2), $w(x)$ is a mathematical window function, which is vanishing for any $|x| > L/2$, such as a rectangular step window, and we normalize the entire field profile by $\max(|w(x)\mathbf{E}_{\text{ideal}}|)$ such that at no point is the amplitude of $\mathbf{E}_{\text{windowed}}(x, z = 0)$ greater than E_{inc} . This will correspond to a passive metasurface transmission coefficient $|t| < 1$, avoiding the need for active amplification. It is reasonable to expect that the results of the windowed case should asymptotically approach the idealized perfect penetration as the window grows $L \rightarrow \infty$ and therefore it is interesting to consider how

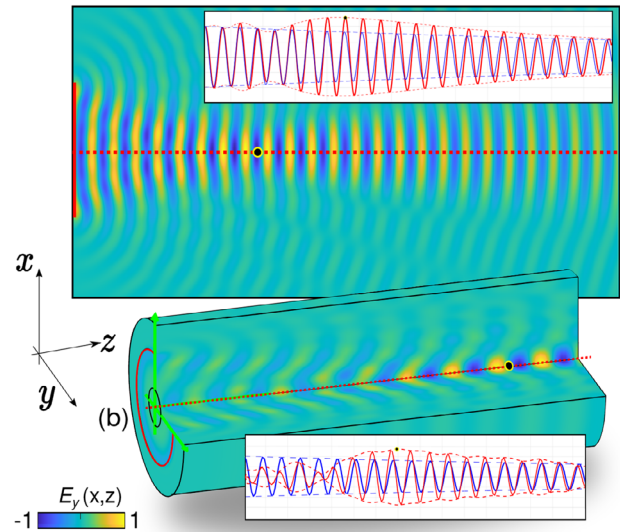


Figure 3. Bullseye metasurface: windowed field profiles. Electric field propagation inside an opaque material when designed boundary conditions (metasurface) are optimized and specified at $z = 0$ corresponding to the windowed versions (window length $L = 1.602$ and $L = 1.308\lambda$ on each case) of a) a complex-argument cosine beam, and b) a complex-argument Bessel beam. The lossy material corresponds again to silicon at HeNe wavelengths. The internal degree of freedom, set to $f = 0.091$ (a) and $f = 0.117$ (b), are optimized to obtain the maximum intensity enhancement inside the opaque material compared to an exponential attenuation (no metasurface). The insets show the field profile for the central position along the z axis as the field propagates inside the opaque material, for the structured windowed cosine beam, i.e. with metasurface (red), and for a non-structured normally incident plane wave, i.e., without metasurface (blue). We find a non-trivial increase in the amplitude of electric field for a wide range of penetration distances that can be effectively tuned for further applications. Maximum intensity enhancement ($I_{\text{with metasurface}}/I_{\text{without}}$) is highlighted with a black dot in both scenarios, and corresponds to 1.65 (a) and 1.76 (b). Numerical simulations were performed using Matlab.

well will the penetration rate work for realistic window sizes. Of course, this windowed profile is no longer a perfect inhomogeneous wave, so we can no longer use simple analytical solutions, and we cannot expect the field inside the opaque material to be translationally invariant along the z -direction. However, because Maxwell's equations are local, one can expect that, locally, the windowed version will be similar to the ideal version $\mathbf{E}_{\text{windowed}} \approx (\max(|w(x)\mathbf{E}_{\text{ideal}}|))^{-1} \mathbf{E}_{\text{ideal}}$ as $w(x) \approx 1$ at least in a neighborhood around $(x, z) = 0$, i.e., near the central axis of the beam, far from the window edges, corresponding to the bullseye proposal. Like a bull's-eye window in the hull of a ship, this metasurface opens up a small region of transmission on an opaque slab.

To study this, we numerically propagate the windowed profile through the opaque medium using a Fourier propagator approach by performing the following steps: we numerically compute the Fourier transform of the field at the plane $z = 0$, followed by an $e^{ik_z z}$ transfer propagator function across the z planes, and finally an inverse Fourier transform on each z plane. The resulting fields are shown in Figure 3, where the intensity profile imposed at $z = 0$ is obtained by windowing the ideal cases of cosine and Bessel beam that were previously shown in Figure 2b,c.

The calculations, which we performed in Matlab, are verified via a Comsol Multiphysics full-wave simulation in the Supporting Information. The window size L was optimized in each case for higher amplitudes along $x = 0$, looking for a trade-off between L being too-small (and thus no opportunity of resembling the original ideal case) or being too-wide (and thus having to normalize the entire profile by a number that is too big, to keep the exponentially growing tails under control). Remarkably, and with no intentionality on our part, the resulting profile shows a focusing behavior, resulting in enhanced field amplitude penetrating in the z -direction along the line $x = 0$, but with low penetration depth elsewhere. This focusing behavior matches well with the fact that the Poynting vector is flowing from the high amplitude edges of the field profile toward the lower amplitude center, at a certain angle, as seen in the ideal cases earlier. Interestingly, it is possible to directionally control this focusing-like behavior of the beam inside the material thanks to the internal degree of freedom f , inherited from Equation (3). Note also that changing the size of the window can also lead to a fine tuning of the profile shape inside the material. If this windowed profile can be set up by a metasurface fabricated at the interface of the opaque material, we may achieve, locally, an enhanced transmission through the material (in our examples from Figure 3 we show up to 76% improved intensity of the field at some points inside the material, with optimization of the internal degree of freedom f and the window size L) for feasible technological applications.

4. Discussion and Future Outlook

A transmitted wave propagating through an opaque material was analytically proven to result from a complex refraction metasurface. This corresponds to a metasurface that generalizes Snell's law to complex angles, by using simultaneous phase and amplitude control. The concept of complex-refraction metasurfaces applies to any wavelength and to any wave-field described by Helmholtz's equation, such as acoustic waves. The main physical explanation is that one can swap the direction of decay from a longitudinal to a transverse direction. This suggests novel methods for transmission through opaque media, moving away from active sources and continuous engineering beam shaping, to a more sustainable approach based on a passive structure metasurface. To solve the nonphysical requirements of infinite energy tails, a solution is presented by windowing the ideal case, corresponding to our proposal of a bullseye metasurface. Having proposed the concept of complex refraction bullseye metasurfaces, further work could look at interesting applications like an in situ wall-mounted metasurface for increased wireless signal transmission through domestic walls or, thanks to the electromagnetic-acoustic formalism analogy, increased sound transmission through "acoustically opaque" (dampening) materials. Note that the phenomenon works for any complex refractive index, whether it is associated to losses, or to lossless but still opaque materials, such as a plasma with a negative but real electric permittivity resulting in purely imaginary refractive index (see Supporting Information). Speculative proposals can therefore be pictured in the context of improved transmission across metals. Medical applications could include the analysis and treatment of malignant cells subcutaneously without damaging the external layer of skin in the human body, without (over)heating

of the interface boundaries, with a proper combination of bullseye metasurface profiles. All the previous technological applications are subordinate to a successful experimental realisation of the required holographic metasurfaces controlling phase and amplitude simultaneously, of which optical and radiofrequency designs exist.^[13,17] Further work for complex refraction metasurfaces is not limited to achieving a zero imaginary part in k_z , but even a negative imaginary part corresponding to exponential increase inside the material, at the cost of even stronger transverse amplitude variation.

Supporting Information

Supporting Information is available from the Wiley Online Library or from the author.

Acknowledgements

S.P.-P. thanks V. Arribas-López for the rendering of the 3D graphic implementation, A. Díaz-Nadales for the helpful suggestion about the Feynman trick and A. Ortega-Arroyo for the fruitful discussion about the potential applications in Health Sciences. F.J.R.-F. thanks N. Engheta for useful discussions. This work was supported by the European Research Council Starting Grant ERC-2016-STG-714151-PSINFONI and EPSRC-2020-20004058-11982 (UK).

Conflict of Interest

The authors declare no conflict of interest.

Data Availability Statement

The data that support the findings of this study are available from the corresponding author upon reasonable request.

Keywords

bullseye metasurface, complex angle, complex Bessel beam, Generalized Snell Law

Received: September 6, 2023
Revised: December 12, 2023
Published online: January 18, 2024

- [1] J. Bertolotti, E. G. van Putten, C. Blum, A. Lagendijk, W. L. Vos, A. P. Mosk, *Nature* **2012**, 491, 232.
- [2] P. Pai, J. Bosch, M. Kühmayer, S. Rotter, A. P. Mosk, *Nat. Photonics* **2021**, 15, 431.
- [3] F. Frezza, N. Tedeschi, *Opt. Lett.* **2012**, 37, 2616.
- [4] P. Baccarelli, F. Frezza, P. Simeoni, N. Tedeschi, *Materials* **2018**, 11, 1595.
- [5] P. Baccarelli, A. Calcaterra, F. Frezza, F. Mangini, N. Ricciardella, P. Simeoni, N. Tedeschi, *Sci. Rep.* **2021**, 11, 15928.
- [6] R. Uppu, M. Adhikary, C. A. Hartevelde, W. L. Vos, *Phys. Rev. Lett.* **2021**, 126, 177402.
- [7] A. Yulaev, S. Kim, Q. Li, D. A. Westly, B. J. Roxworthy, K. Srinivasan, V. A. Aksyuk, *Nat. Nanotechnol.* **2022**, 17, 583.
- [8] H. Li, A. Mekawy, A. Alù, *Phys. Rev. Lett.* **2021**, 127, 014301.

- [9] P. Lalanne, S. Astilean, P. Chavel, E. Cambriil, H. Launois, *Opt. Lett.* **1998**, *23*, 1081.
- [10] E. Silberstein, P. Lalanne, J.-P. Hugonin, Q. Cao, *J. Opt. Soc. Am. A* **2001**, *18*, 2865.
- [11] H.-T. Chen, A. J. Taylor, N. Yu, *Rep. Prog. Phys.* **2016**, *79*, 076401.
- [12] J. Hu, S. Bandyopadhyay, Y. hui Liu, L. yang Shao, *Front. Phys.* **2021**, *8*, 586087.
- [13] O. Quevedo-Teruel, H. Chen, A. Díaz-Rubio, G. Gok, A. Grbic, G. Minatti, E. Martini, S. Maci, G. V. Eleftheriades, M. Chen, N. I. Zheludev, N. Papisimakis, S. Choudhury, Z. A. Kudyshev, S. Saha, H. Reddy, A. Boltasseva, V. M. Shalaev, A. V. Kildishev, D. Sievenpiper, C. Caloz, A. Alù, Q. He, L. Zhou, G. Valerio, E. Rajo-Iglesias, Z. Sipus, F. Mesa, R. Rodríguez-Berral, F. Medina, et al., *J. Opt.* **2019**, *21*, 073002.
- [14] N. Yu, P. Genevet, M. A. Kats, F. Aieta, J.-P. Tetienne, F. Capasso, Z. Gaburro, *Science* **2011**, *334*, 333.
- [15] N. Yu, F. Capasso, *Nat. Mater.* **2014**, *13*, 139.
- [16] W. T. Chen, A. Y. Zhu, F. Capasso, *Nat. Rev. Mater.* **2020**, *5*, 604.
- [17] P. Genevet, F. Capasso, *Rep. Prog. Phys.* **2015**, *78*, 024401.
- [18] P. Zhang, B. Fang, T. Zhao, L. Ke, X. Ma, C. Li, Z. Hong, X. Jing, *Results Phys.* **2023**, *46*, 106328.
- [19] A. C. Overvig, S. Shrestha, S. C. Malek, M. Lu, A. Stein, C. Zheng, N. Yu, *Light: Sci. Appl.* **2019**, *8*, 92.
- [20] G. Gok, A. Grbic, in *2014 IEEE Antennas and Propagation Society International Symposium (APSURSI)*, IEEE, Piscataway, NJ **2014**, pp. 765–766.
- [21] F. J. Rodríguez-Fortuño, G. Marino, P. Ginzburg, D. O'Connor, A. Martínez, G. A. Wurtz, A. V. Zayats, *Science* **2013**, *340*, 328.
- [22] M. Born, E. Wolf, A. B. Bhatia, P. C. Clemmow, D. Gabor, A. R. Stokes, A. M. Taylor, P. A. Wayman, W. L. Wilcock, *Principles of Optics: Electromagnetic Theory of Propagation, Interference and Diffraction of Light*, 7th ed., Cambridge University Press, Cambridge **1999**.
- [23] A. Y. Bekshaev, K. Y. Bliokh, F. Nori, *Opt. Express* **2013**, *21*, 7082.
- [24] D. E. Aspnes, A. A. Studna, *Phys. Rev. B* **1983**, *27*, 985.
- [25] J. Durnin, *J. Opt. Soc. Am. A* **1987**, *4*, 651.
- [26] A. Ortiz-Ambriz, S. Lopez-Aguayo, Y. V. Kartashov, V. A. Vysloukh, D. Petrov, H. Garcia-Gracia, J. C. Gutiérrez-Vega, L. Torner, *Opt. Express* **2013**, *22*, 22221.
- [27] A. Bencheikh, S. Chabou, O. C. Boumeddine, H. Bekkis, A. Benstiti, L. Beddiaf, W. Moussaoui, *J. Opt. Soc. Am. A* **2020**, *37*, C7.